Efficacy of passive sampler collection for atmospheric NO_2 isotopes under simulated environmental conditions

Justin G. Coughlin* [iD], Zhongjie Yu and Emily M. Elliott

Department of Geology and Environmental Science, University of Pittsburgh, Pittsburgh, PA 15260, USA

RATIONALE: Nitrogen oxides or NO_x ($NO_x = NO + NO_2$) play an important role in air quality, atmospheric chemistry, and climate. The isotopic compositions of anthropogenic and natural NO_2 sources are wide-ranging, and they can be used to constrain sources of ambient NO_2 and associated atmospheric deposition of nitrogen compounds. While passive sample collection of NO_2 isotopes has been used in field studies to determine NO_x source influences on atmospheric deposition, this approach has not been evaluated for accuracy or precision under different environmental conditions.

METHODS: The efficacy of NO_2 passive sampler collection for NO_2 isotopes was evaluated under varied temperature and relative humidity (RH) conditions in a dynamic flux chamber. The precision and accuracy of the filter NO_2 collection as nitrite (NO_2^-) for isotopic analysis were determined using a reference NO_2 gas tank and through inter-calibration with a modified EPA Method 7. The bacterial denitrifer method was used to convert 20 μM of collected NO_2^- or nitrate (NO_3^-) into N_2O and was carried out on an Isoprime continuous flow isotope ratio mass spectrometer.

RESULTS: $\delta^{15}N$-NO_2 values determined from passive NO_2 collection, in conditions of 11–34 °C, 1–78% RH, have an overall accuracy and precision of ±2.1 ‰, and individual run precision of ±0.6 ‰. $\delta^{18}O$-NO_2 values obtained from passive NO_2 sampler collection, under the same conditions, have an overall precision of ± 1.3 ‰.

CONCLUSIONS: Suitable conditions for passive sampler collection of NO_2 isotopes are in environments ranging from 11 to 34 °C and 1 to 78% RH. The passive NO_2 isotope measurement technique provides an accurate method to determine variations in atmospheric $\delta^{15}N$-NO_2 values and a precise method for determining atmospheric $\delta^{18}O$-NO_2 values. The ability to measure NO_2 isotopes over spatial gradients at the same temporal resolution provides a unique perspective on the extent and seasonality of fluctuations in atmospheric NO_2 isotopic compositions. Copyright © 2017 John Wiley & Sons, Ltd.

Nitrogen oxides ($NO + NO_2 = NO_x$) play an important role in local and regional atmospheric chemistry, air quality, and climate.[1,2] NO_x is a precursor to tropospheric ozone (O_3) through the photodissociation (≤400 nm) of NO_2 to both NO and a ground-state oxygen [O(^{3}P)].[2–4] The O(^{3}P) atom is able to react with atmospheric oxygen (O_2) to produce O_3 in the atmosphere. This is especially prevalent in areas of high NO_x concentrations,[5] which can then create public health issues as NO_x and O_3 are harmful to the respiratory systems of children and asthmatic individuals.[6,7] In addition, an excited oxygen atom [O(^{1}D)] is produced through O_3 photolysis (<310 nm), which can react with water vapor ($H_2O_{(g)}$) in the troposphere, or hydronium ions (H_3O^+) in dense gas, to form the hydroxyl radical (·OH).[4,8] The formation of ·OH has important implications for the production of nitric acid (HNO_3), which can deposit back to the Earth's surface and lead to water quality degradation, acidification of soils, and the eutrophication of waterways.[9]

Anthropogenic sources of NO_x, such as vehicles, power plants, and other industrial processes, account for nearly 85% of the NO_x emissions inventory in the contiguous United States.[10] Natural sources of NO_x (e.g. microbial processes, lightning) are also significant NO_x emissions sources,[11,12] but large uncertainties for these sources currently exist in the nationwide NO_x emission inventory, ranging from ±20 to 50%.[9,12] The conservation of the nitrogen atom between NO_x sources and sinks allows for the determination of NO_x source apportionments to ecosystems using $\delta^{15}N$ signatures. The $\delta^{15}N$ values of NO_x from anthropogenic and natural sources have recently become more widely documented and span a large range (–49 to +26 ‰), depending on the NO_x emission source.[13–23] In addition, recent experimental and modeling efforts have focused on determining kinetic and equilibrium isotope fractionation associated with the tropospheric oxidation of NO_x to nitrate (NO_3^-) to facilitate tracing the land-atmosphere reactive NO_x cycle using $\delta^{15}N$ signatures.[24–26] To date, the $\delta^{15}N$ values of NO_x and depositional NO_3^- have been used to estimate the contribution of NO_x emissions sources to dry and wet NO_3^- deposition,[27–32] historical nitrogen deposition in lake and ice cores,[33–35] and nutrient sourcing of plants.[19,22,36]

* *Correspondence to:* J. G. Coughlin, Department of Geology and Environmental Science, University of Pittsburgh, 4107 O'Hara St, 200 SRCC, Pittsburgh, PA 15260, USA.
E-mail: jgc23@pitt.edu

Rapid Commun. Mass Spectrom. 2017, 31, 1211–1220

1211

A variety of measurement techniques have been used to determine the $\delta^{15}N$ values of both NO_x sources and ambient NO_2 or NO_x, including denuder tubes coated with NaOH/guiacol or KOH/guiacol,[19,20,26] active bubbler collections (NO, NO_2, or NO_x) that utilize triethanolamine (TEA), NaOH/KMnO$_4$, NaOH/H$_2$O$_2$, or H$_2$SO$_4$/H$_2$O$_2$ absorbing solutions,[15,16,18,37] and passive diffusion samplers.[17,38,39] Each isotope collection technique has its own benefits or limitations. In particular, $NO_{2(g)}$ diffusion samplers create a concentration gradient between ambient air and air inside the tube. As $NO_{2(g)}$ diffuses through physical barriers, such as diffusive caps or screens, ambient $NO_{2(g)}$ is then adsorbed to a filter impregnated with $NO_{2(g)}$ collection solutions such as TEA or NaI/NaOH solutions. Filters are then eluted with deionized water to collect $NO_2^-_{(aq)}$ ions in solution for subsequent concentration and isotopic analyses.[17,38] In a pioneering study, Redling *et al.* utilized isotope mixing models on passively collected $NO_{2(g)}$ to determine source apportionment from a variety of sources, with the assumption that $NO_{x(g)}$ quickly oxidized to $NO_{2(g)}$ over short spatial gradients away from mobile sources.[38] Felix and Elliott examined variations in $\delta^{15}N\text{-}NO_2$ values with sampler deployment height, deployment length, and in areas with different NO_x sources (e.g., livestock, vehicles, etc.) using Ogawa $NO_{2(g)}$ samplers.[17] In another report, Dahal and Hastings in a study of $\delta^{15}N\text{-}NO_2$ and $\delta^{15}N\text{-}NO_x$ values determined from passive sampler collection concluded that: (1) the values are indicative of a mixture of sources, (2) collection of $NO_{2(g)}$ isotopes may not necessarily be equivalent to $NO_{x(g)}$ isotopes from sources, and (3) passive samplers have a precision of <1 ‰ amongst samples.[40]

Although passive sampler collection of $NO_{2(g)}$ has been shown to be a robust tool for evaluating $\delta^{15}N\text{-}NO_2$ fluctuations and NO_x source mixing,[38,40] a quantitative assessment of the accuracy and precision associated with the filter collection and subsequent $\delta^{15}N\text{-}NO_2$ analysis is still lacking. Previous investigations focusing on $NO_{2(g)}$ concentration analysis have identified ambient temperature, relative humidity (referred to as RH for the rest of the paper), and wind speed as the key factors affecting the $NO_{2(g)}$ uptake efficiency of passive samplers.[41] For example, RH has been found to be the most important environmental factor influencing the effective sampling rate of passive $NO_{2(g)}$ samplers due to the inefficiency of TEA as an absorbent at low relative humidities.[42–44] However, it is currently unknown if changes in the $NO_{2(g)}$ uptake efficiency induced by varying environmental conditions can cause fractionation of $NO_{2(g)}$ isotopes during passive $NO_{2(g)}$ collection. Since passive samplers are distinctive monitoring tools that can be deployed in multiple locations to collect $NO_{2(g)}$ with a desired temporal resolution, it is vital to determine whether varying environmental conditions influence the $\delta^{15}N\text{-}NO_2$ values determined by using passive samplers.

In this study, the efficacy of the Ogawa passive sampler collection for $NO_{2(g)}$ isotopes was evaluated under varying simulated conditions in a dynamic flux chamber. The precision and accuracy of the $\delta^{15}N\text{-}NO_2$ analysis were determined using a reference $NO_{2(g)}$ tank and through inter-calibration with a modified EPA Method 7 originally designed for stationary NO_x sources. The results of this study have important implications for $NO_{2(g)}$ isotope collection methods because of the passive sampler method's simplicity, inexpensiveness, and time-integrated collection of $NO_{2(g)}$ isotopes.

EXPERIMENTAL

Ogawa filter assembly

Passive samplers are effective for determining ambient air concentrations of nitrogen-containing molecules (e.g. $NO_{2(g)}$, $NH_{3(g)}$, $HNO_{3(g)}$), are inexpensive, require little maintenance, and do not require electricity.[27,38,45–48] In particular, the Ogawa passive sampler body (Ogawa & Company, Pompano Beach, FL, USA) consists of a double-sided passive diffusion design with diffusion end caps on both sides, followed by a stainless steel screen, a 14.5 mm cellulose filter impregnated with a 10% TEA adsorbing solution, followed by another stainless steel screen, and then a retainer ring. In addition, the sampler bodies are covered by an opaque, plastic shelter to prevent influence from the sun or rainfall.

Ogawa fractionation tests

A cylindrical dynamic flux chamber (15 cm height and 18 cm i.d.) was used to simulate varying environmental conditions and their potential influence on $NO_{2(g)}$ isotope collection onto the Ogawa passive samplers (Fig. 1). The chamber was made of 5 mm thick transparent acrylic plastic and lined with 0.05 mm thick Teflon film. A low-speed electric fan was installed inside the chamber to aid in-air mixing. The air temperature and RH in the chamber headspace were continuously measured using a HOBO sensor (Onset Computer Corporation®, Bourne, MA, USA) at 1 min intervals. A NIST-traceable reference gas tank containing 104.9 ppmv $NO_{2(g)}$ balanced in air (Matheson, Montgomeryville, PA, USA) was connected to the flux

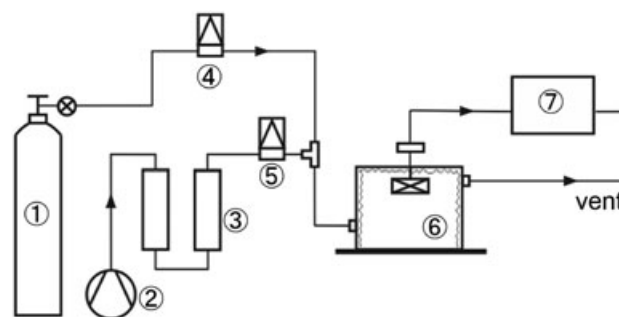**Figure 1.** Passive sampler collection setup. An $NO_{2(g)}$ reference gas tank (1) and a vacuum pump (2) were connected to the chamber (6) via Teflon tubing. Passive filter assemblies were placed inside the chamber (6). Zero-air passes through columns (3) to remove $NO_{x(g)}$, $O_{3(g)}$, and VOCs and then passes through a humidity control device (3). Air flow from the reference gas tank and zero-air were controlled by mass flow controllers ((4) and (5), respectively). $NO_{2(g)}$ concentrations inside the chamber were analyzed by a chemiluminescence $NO\text{-}NO_2\text{-}NO_x$ analyzer (Thermo Environmental Instruments, Franklin, MA, USA) (7). Excess air flow exited the chamber via Teflon tubing through the vent.

chamber via 0.25" Teflon tubing and the flow rate was controlled using a mass flow controller [0–200 standard cubic centimeters per minute (SCCM), SmartTrak 50; Sierra Instruments, Monterey, CA, USA] (Fig. 1). A zero-air flow free of $NO_{x(g)}$, $O_{3(g)}$, and volatile organic compounds (VOCs) was produced by passing a pressurized ambient air flow through columns of activated carbon and Purafil® and was controlled by a mass flow controller [0–10 standard liters per minute (SLPM), SmartTrak 50] to dilute the $NO_{2(g)}$ flow to desired $NO_{2(g)}$ concentrations (Fig. 1). Wind velocity and air flow were measured inside the chamber using a HOBO wind speed sensor (Onset Computer Corporation) and a PMA90 digital anemometer (Pyle Audio Inc., Brooklyn, NY, USA), but were not detectable at the accuracy resolution of the instrumentation.

The environmental conditions simulated in this study included varied temperature and RH levels and are summarized in Table 1. All experiments were conducted under dark conditions in order to prevent UV light interaction with $NO_{2(g)}$, which could result in $NO_{2(g)}$ dissociating to $NO_{(g)}$. The temperature and RH could not be controlled at a high sensitivity in the experimental design so three different levels of temperature and RH were designated: low, moderate, and high. Low-temperature levels were designated as 10–13°C, moderate was 22–23°C, and high was 33–34°C. Low RH conditions were designated as <5%, moderate was 20–70%, and high was >70%. The chamber temperature was varied either by heating the chamber exterior using a self-limiting heating cable or by placing the chamber into a refrigerator during sample collection. To vary the RH in the chamber headspace, the zero-air flow was forced to pass through either a drierite column, to remove moisture, or a 500-mL gas-washing bottle containing 250 mL deionized water, to create moisture, before the zero-air and $NO_{2(g)}$ flows were mixed. Moderate temperature and RH conditions were based on ambient laboratory conditions and did not utilize a control method (e.g. heating coil, refrigerator, drierite column, or gas washing bottle). The Teflon tubing was flushed with inert $N_{2(g)}$ prior to sample collection in order to remove any impurities within the tubing system.

Ogawa passive samplers were deployed inside the flux chamber in duplicate (2 samplers, 4 filters) for seven separate sample collections and were covered by an opaque shelter to simulate field deployment setup. Two laboratory blanks were collected on the same day as the experiments. Little to no

$NO_2^-_{(aq)}$ (<0.02 mg L^{-1} $NO_2^-_{(aq)}$) was present on all laboratory blanks. The samplers were deployed for 12 h inside the flux chamber under simulated temperature, RH, and $NO_{2(g)}$ concentration conditions. Upon collection completion, individual filters were removed from the passive sampler, transferred to a polyethylene sampling vial (Fisher Scientific, Waltham, MA, USA), and were then stored at –20°C until subsequent concentration and isotopic analyses.

Concentration analyses and ppbv calculation

Filters were eluted with 5 mL of 18.2 MΩ MilliQ water (EMD MilliPore Corp., Kankakee, IL, USA) to produce $NO_2^-_{(aq)}$ ions. Filter eluent concentrations of $NO_2^-_{(aq)}$ were analyzed on a Thermo Evolution 60S UV-Visible spectrophotometer (Thermo Fisher Scientific, Skokie, IL, USA). Theoretical $[NO_2^-_{(aq)}]$ (mg L^{-1}) calculations were back-calculated for each experiment using a temperature and RH dependence equation developed by Ogawa & Co.:[49]

$$[NO_2^-{}_{(aq)}]_t = \frac{\left([NO_{2(g)}]_v * t\right)}{(10,000/(0.677*P*RH) + (2.009*T) + 89.8)} \quad (1)$$

$$* \frac{1\ mg}{1,000,000\ ng} * E * \frac{1000\ mL}{1\ L} * V_C$$

where $[NO_2^-_{(aq)}]_t$ is the theoretical $NO_2^-_{(aq)}$ concentration (mg L^{-1}) eluted from a filter, $[NO_{2(g)}]_v$ is the $NO_{2(g)}$ concentration (ppbv) in the chamber, t is the time of filter exposure (min), P is a dimensionless vapor pressure coefficient corresponding to a temperature,[49] RH is the average RH inside the chamber (%), T is the average temperature inside the chamber (°C), E is the elution volume (5 mL), and V_C is a stoichiometric conversion that is used to convert the $NO_2^-_{(aq)}$ measured in the total solution to the initial solution to adjust for reagent volume addition needed for concentration analyses. Collection efficiencies were then calculated for each experiment by comparing the measured $[NO_2^-_{(aq)}]$ with the theoretical concentrations.

Reference gas tank collection using modified EPA Method 7

A modified version of the US EPA Method 7 (Determination of Nitrogen Oxide Emissions from Stationary Sources) was utilized to collect $NO_{2(g)}$ from the 104.9 ppmv $NO_{2(g)}$ gas tank (hereafter referred to as the reference gas tank).[50] This

Table 1. Environmental conditions tested inside the chamber with corresponding collection dates, collection time (min), $NO_{2(g)}$ concentration (ppbv), relative humidity (RH, %), temperature (°C), flow rate [slpm (standard liters per minute)] conditions, and the respective settings

Test	Date	Collection period (min)	NO₂ conc. (ppbv)	Temp. (°C)	RH (%)	Flow rate (slpm)	Setting
1	5/27/2016	720	373	23.0 ± 0.3	33.3 ± 0.8	7.0	Moderate T, Moderate RH
2	5/28/2016	720	373	23.2 ± 0.3	1.3 ± 1.1	7.0	Moderate T, Low RH
3	5/29/2016	720	373	22.4 ± 0.2	77.7 ± 0.9	7.0	Moderate T, High RH
4	6/1/2016	720	373	32.5 ± 0.8	1.3 ± 1.2	7.0	High T, Low RH
5	6/2/2016	720	418	11.2 ± 1.2	1.3 ± 1.8	3.0	Low T, Low RH
6	1/4/2017	720	373	33.7 ± 0.1	20.9 ± 0.6	7.0	High T, Moderate RH
7	1/5/2017	720	418	12.5 ± 0.7	64.3 ± 1.6	3.0	Low T, Moderate RH

method has been described in detail by Walters *et al*. and Felix *et al*.[13,14,16] Briefly, samples from the tank were collected in evacuated 1-L borosilicate bulbs (Sigma Aldrich, St. Louis, MO, USA) which were connected to tubing attached to the reference gas tank. Samples were collected for approximately 1 min after which the stopcock connecting the bulb to the tank was closed. The sampling bulbs contained 10 mL of a $NO_{x(g)}$-absorbing solution, made using 2.8 mL of concentrated sulfuric acid (H_2SO_4) (Fisher Scientific, Waltham, MA, USA) and 0.6 mL of 30% hydrogen peroxide (H_2O_2) (Sigma Aldrich), which was then diluted to 1 L using 18.2Ω MilliQ water. The absorbing solution traps $NO_{2(g)}$ in the form of $NO_2^-{}_{(aq)}$ then oxidizes it further to $NO_3^-{}_{(aq)}$, allowing for concentration and isotopic composition analyses. Tank samples were collected in triplicate. After $NO_{2(g)}$ collection from the tank, the samples were kept in a dark, ambient temperature environment for 1 week with daily shaking to allow for complete oxidation of $NO_2^-{}_{(aq)}$ to $NO_3^-{}_{(aq)}$. The headspace of each bulb was subsequently analyzed for any remaining NO_x concentration using a Chemiluminescence i17 NO-NO_2-NO_x analyzer (Thermo Environmental Instruments, Franklin, MA, USA). The remaining headspace in the bulbs was determined to have concentrations of ≤2.5 ppbv NO_x, indicating a > 99.9% collection efficiency. The absorbing solution was transferred to plastic bottles and neutralized using 1 mL of sodium bicarbonate ($NaHCO_3$) (Sigma Aldrich). Blank samples of the collection solution were analyzed and yielded no background $NO_3^-{}_{(aq)}$ presence during the isotopic analyses.

Isotopic analyses

Isotopic analyses of NO_2 filter eluents and neutralized reference gas tank samples were conducted using the bacterial denitrifier method. $NO_2^-{}_{(aq)}$ or $NO_3^-{}_{(aq)}$ (20 nmol) was converted into $N_2O_{(g)}$ utilizing a denitrifying bacteria, *P. aureofaciens*.[51,52] The filter samples were analyzed 3–5 times and reference gas tank samples were analyzed 8 times for $\delta^{15}N$ and $\delta^{18}O$ values using an Isoprime Trace Gas and Gilson GX-271 autosampler coupled to a continuous flow isotope ratio mass spectrometer (IsoPrime Ltd, Stockport, UK) at the University of Pittsburgh *Regional Stable Isotope Laboratory for Earth and Environmental Science Research* (Pittsburgh, PA, USA). Nitrogen and oxygen isotope ratios are reported as δ values in parts per thousand relative to atmospheric N_2 and VSMOW (Vienna Standard Mean Ocean Water), respectively, as:

$$\delta(‰) = \left(\frac{(R)sample}{(R)standard} - 1 \right) \quad (2)$$

where R denotes the ratio between the heavy and light isotopes (e.g. $^{15}N/^{14}N$ and $^{18}O/^{16}O$). The raw $\delta^{15}N$ and $\delta^{18}O$ values were corrected using a $NO_2^-{}_{(aq)}$ standard, RSIL-20 (USGS-Reston, $\delta^{15}N$-RSIL-20 = –79.6 ‰ vs air, $\delta^{18}O$-RSIL-20 = +4.5 ‰ vs VSMOW),[53] the international reference standards USGS-34 and IAEA-N3, and an internal nitrite reference standard ($\delta^{15}N$ = –27.4 ‰ vs air) calibrated by the aforementioned standards and inter-laboratory comparisons. RSIL-20 was used in order to improve the calibration capability for the low $\delta^{15}N$-NO_2 tank samples, and to allow

Table 2. Measured filter eluent concentrations, theoretical filter eluent concentrations, and associated data needed to calculate theoretical concentrations

Setting	Chamber $NO_{2(g)}$ conc. (ppbv)	Temp. (°C)	RH (%)	Time (min)	P (dimensionless)[a]	Theoretical conc. (mg L^{-1} $NO_{2(aq)}$)	Measured conc. (mg L^{-1} $NO_{2(aq)}$)	Collection efficiency (%)
Moderate T, Moderate RH	373	23.0	33.3	720	0.938	0.84	1.06	125
Moderate T, Low RH	373	23.2	1.3	720	0.938	0.74	0.92	124
Moderate T, High RH	373	22.4	77.7	720	0.9587	1.00	1.09	110
High T, Low RH	373	32.5	1.3	720	0.7385	0.84	0.97	116
Low T, Low RH	417	11.2	1.3	720	1.1794	0.68	1.01	148
High T, Moderate RH	373	33.7	20.9	720	0.7198	0.90	0.95	106
Low T, Moderate RH	418	12.5	64.3	720	1.1412	0.99	1.10	111

[a]The vapor pressure coefficient (P) is used from the Ogawa protocol.[9]

for a secondary correction to the $\delta^{18}O$ values of nitrite samples calibrated by nitrate standards.[53] This correction was applied to sample $\delta^{18}O$ values by subtracting the average measured $\delta^{18}O$-NSIL-20 value from its true value for each run, and then adding the difference to the sample $\delta^{18}O$ values.[40,53] The average correction factor across all isotopic composition analysis runs was $+28.3 \pm 0.5$ ‰ ($n = 17$). Standard replicates had an average standard deviation (σ) of ≤ 0.25‰ for $\delta^{15}N$ values and ≤ 0.5‰ for $\delta^{18}O$ values.

Statistical analyses

Analysis of variance (ANOVA) tests, regression analyses, and t tests were conducted in TIBCO Spotfire S+® 8.2.[54] The groupings of filter collections for ANOVA tests were: (1) all filter samples (Tests 1–7, Table 1), (2) moderate T, varying RH conditions (Tests 1–3, Table 1), (3) low T, varying RH conditions (Tests 5 and 7, Table 1), (4) varying T, low RH conditions (Tests 2, 4, and 5, Table 1), (5) varying T conditions, moderate RH (Tests 1, 6, and 7, Table 1), and (6) high T, varying RH conditions (Tests 4 and 6, Table 1). In addition, two sample t tests (assuming unequal variances) were conducted to compare reference gas tank samples against all the groupings used in the ANOVA analyses. An alpha (α) level of 0.05 was used for both ANOVA and t tests.

RESULTS AND DISCUSSION

Collection results

The theoretical concentrations for the NO$_{2(g)}$ collection solution (reference gas tank) were 26.2 ppm NO$_3^-{}_{(aq)}$, assuming 100% collection. The NO$_2^-{}_{(aq)}$ concentration of the filter eluents ranged from 0.92 to 1.1 mg L^{-1} NO$_2^-{}_{(aq)}$ with an average of 1.01 ± 0.06 mg L^{-1} NO$_2^-{}_{(aq)}$ (Table 2). The theoretical concentrations back-calculated from the Ogawa protocol ranged from 0.68 to 1.0 mg L^{-1} NO$_2^-{}_{(aq)}$ with an average of

0.86 ± 0.11 mg L^{-1} NO$_2^-{}_{(aq)}$ (Table 2).[49] The collection efficiency (%) for each environmental condition tested ranged from 106 to 148% with an average of $120 \pm 13\%$ (Table 2). Collection efficiencies in excess of 100% may be due to: (1) inaccuracy in the dimensionless vapor pressure coefficient (P) used in Eqn. (2) that is assumed based on temperature, or (2) the Ogawa calculation not being entirely applicable to well-mixed, enclosed settings (e.g., small chambers). Since the laboratory blanks had concentrations (<0.02 mg L^{-1} NO$_2^-{}_{(aq)}$) near the instrument detection limit, we rule out additional NO$_{2(g)}$ collected by sample filters as a potential cause of >100% collection efficiencies. In addition, given that turbulence was undetectable in the chamber (i.e., turbulence could shorten the total diffusion path), this indicates that higher effective sampling rates from turbulent conditions were not the cause of >100% collection efficiency.[55] Together, this suggests that overestimated collection efficiencies are probably due to uncertainty in the theoretical concentration calculation, rather than previously documented environmental or contamination factors in studies using open NO$_{2(g)}$ diffusion tubes.[55–58]

The $\delta^{15}N$-NO$_2$ values determined for the reference gas tank ranged from –39.5 to –40.0 ‰ ($n = 3$), with an average of -39.8 ± 0.2 ‰ (Fig. 2). The average $\delta^{15}N$ value (–39.8 ‰) is hereafter used as the reference gas tank value for comparison against passive filter sample collections. $\delta^{18}O$-NO$_2$ values could not be definitively determined for the reference gas because of the inability to determine reagent interference magnitude. There is an oxygen addition on the initial NO$_{2(g)}$ trapping to NO$_2^-{}_{(aq)}$ which is then oxidized to NO$_3^-{}_{(aq)}$ by an oxygen from either H$_2$O, H$_2$O$_2$, or H$_2$SO$_4$ in the absorbing solution. This additional oxygen could not be accounted for because blank collection solutions did not yield N$_2$O$_{(g)}$ in the vial headspace. The reference gas tank $\delta^{18}O$-NO$_2$ values were 12.7 ± 0.2 ‰, but since the additional oxygen $\delta^{18}O$ value could not be determined, the tank isotope values were not statistically compared to the filter collection values (Fig. 2).[53]
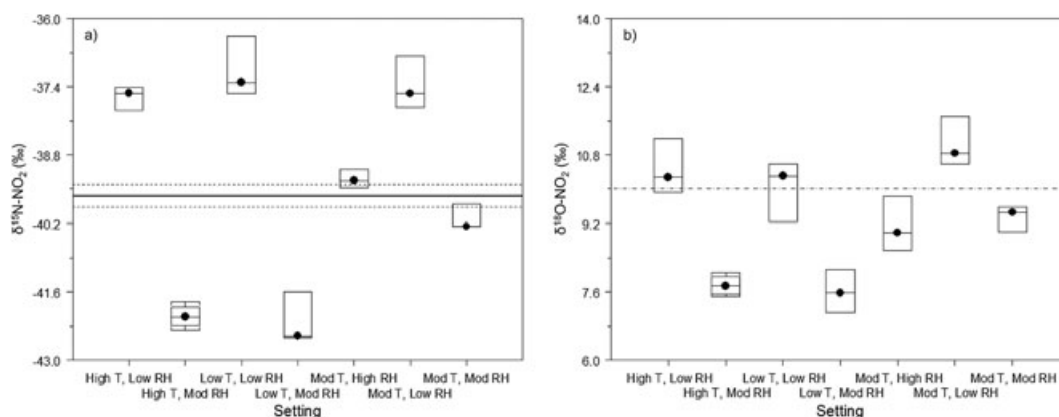

Figure 2. Box and whisker plots showing (a) the range of $\delta^{15}N$-NO$_2$ values measured using Ogawa NO$_{2(g)}$ filters under varying temperature (T) and relative humidity (RH) conditions and (b) range of $\delta^{18}O$-NO$_2$ values measured using Ogawa NO$_{2(g)}$ filters under varying temperature (T) and relative humidity (RH) conditions. Black circles with lines represent the median isotope value of filter samples for a particular environmental setting. The solid black line in (a) represents the average $\delta^{15}N$-NO$_2$ value determined from the reference gas tank. Dashed lines in (a) represent the standard deviation in $\delta^{15}N$-NO$_2$ values from the reference gas tank. The dashed line with dots in (b) represents the average $\delta^{18}O$-NO$_2$ value obtained from filter tests across all environmental conditions.

The δ^{15}N-NO$_2$ values determined from the filter eluents ranged from –36.5 to –42.5 ‰ with an average of –39.5 ± 2.1 ‰ across all simulated environmental conditions (Fig. 2). The δ^{18}O-NO$_2$ values determined from the filter eluents ranged from 7.1 to 11.7 ‰ with an average of 9.3 ± 1.3 ‰ across all simulated environmental conditions (Fig. 2).

Environmental condition effects

Temperature variations had an effect on the concentration collection by passive samplers, but not on isotope collections (Fig. 3). While isotope effects were observed when the temperature was varied, these effects were due to variations in RH rather than to differences in temperature. The average [NO$_2^-$$_{(aq)}$] collected in varied T (11–33°C), low RH conditions was 0.97 ± 0.04 mg L^{-1} NO$_2^-$$_{(aq)}$. The average [NO$_2^-$$_{(aq)}$] collected in varied T (13–34°C), moderate RH conditions was 1.03 ± 0.06 mg L^{-1} NO$_2^-$$_{(aq)}$. There is a significant, negative correlation between the temperature measurements in the chamber and the measured filter NO$_2^-$$_{(aq)}$ eluent concentrations (Fig. 3). The correlation indicates that higher temperatures are associated with less effective passive sampling rates.

The RH conditions in the chamber had an effect on both concentrations and δ^{15}N-NO$_2$ values (Fig. 3). The average [NO$_2^-$$_{(aq)}$] collected in moderate T, varied RH conditions was

1.02 ± 0.07 mg L^{-1} NO$_2^-$$_{(aq)}$. In this experiment, the eluent concentration collection efficiencies showed >100% collection for all environmental conditions, and increasing RH conditions resulted in increased NO$_2^-$$_{(aq)}$ concentrations (Fig. 3). There is a significant, positive correlation ($r^2 = 0.71$, $p < 1$ E^{-15}) between the RH conditions measured in the chamber and the measured filter eluent [NO$_2^-$$_{(aq)}$] (Fig. 3). This correlation demonstrates that increasing RH conditions result in higher effective sampling rates.

The average δ^{15}N-NO$_2$ value from filter collections under varied T, low RH conditions was –37.4 ± 0.4 ‰ ($n = 9$). Under varied T, moderate RH conditions, the average δ^{15}N-NO$_2$ value from filter collections was –41.5 ± 1.0 ‰ ($n = 10$). The average δ^{18}O-NO$_2$ value from filter collections under varied T, low RH conditions was 10.5 ± 0.7 ‰ ($n = 9$). Under varied T, moderate RH conditions, the average δ^{18}O-NO$_2$ value from filter collections was 8.2 ± 0.8 ‰ ($n = 10$). The reference gas tank δ^{15}N-NO$_2$ values were statistically different from all the varied T passive sampler δ^{15}N-NO$_2$ values, but the passive sampler δ^{15}N-NO$_2$ values were not always statistically different from one another. There was a significant difference ($p < 0.0001$ and <0.05 for low RH and moderate RH conditions, respectively) between the average δ^{15}N-NO$_2$ value from the reference gas tank and the average passive sampler δ^{15}N-NO$_2$ value under varied temperatures. In contrast, ANOVA analyses indicated that the δ^{15}N-NO$_2$ values (filter collections under varied T, low RH conditions) did not have

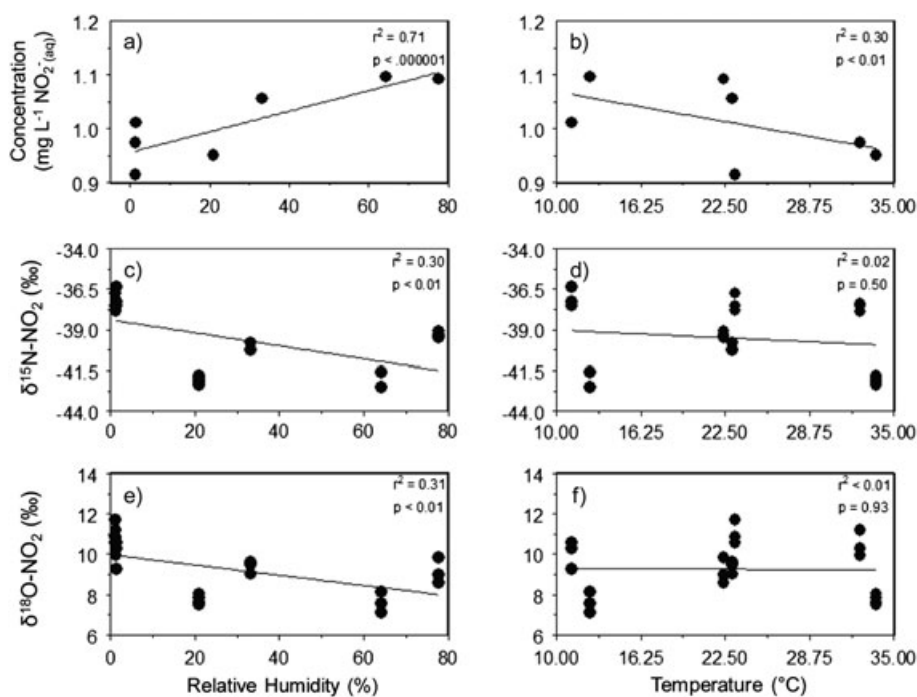**Figure 3.** Linear regressions between (a) average relative humidity in the chamber vs. measured filter eluent NO$_2^-$$_{(aq)}$ concentration, (b) average temperature in the chamber vs. measured filter eluent NO$_2^-$$_{(aq)}$ concentration, (c) average relative humidity in the chamber vs. δ^{15}N-NO$_2$ values, (d) average temperature in the chamber vs. δ^{15}N-NO$_2$ values, (e) average relative humidity in the chamber vs. δ^{18}O-NO$_2$ values, and (f) average temperature in the chamber vs. δ^{18}O-NO$_2$ values. R^2 and p values are also shown. In (a) and (b), all circle symbols are an average ($n = 3$–4). In (a), (c), and (e), temperature and flow rates were not held constant. In (b), (d), and (f) relative humidities and flow rates were not held constant.

a significant difference ($p = 0.21$) amongst each other. The δ^{15}N-NO$_2$ values from passive sampling collections in varied T, moderate RH conditions did, however, show significant differences between each another ($p < 0.0001$).

Due to limitations of the experimental setup, the ambient laboratory RH conditions in the chamber could not be precisely controlled when the temperature was varied, so combined environmental effects occurred during varied T, moderate RH collections. Moderate RH conditions (21–64%) were more widely ranging than low RH conditions (1.3%), and ANOVA analyses of both settings indicate that there was only a significant difference amongst samples when RH was also varied. The lack of a significant temperature effect on both δ^{15}N-NO$_2$ and δ^{18}O-NO$_2$ values is also demonstrated by the absence of a correlation between temperature and isotopic compositions (Fig. 3). While there were differences between average δ^{15}N-NO$_2$ values from the reference gas tank and average δ^{15}N-NO$_2$ values from filter collections under varied T conditions, these effects were confounded by RH effects rather than being caused by temperature effects.

We observed minor isotopic fractionation (≤ 2.5 ‰) across all variations in RH conditions and preferential ^{15}N diffusion under extreme RH conditions (1.3 and 78%). The average δ^{15}N-NO$_2$ value of filter samples collected in moderate T, varied RH conditions (1.3–77.7%) was -38.4 ± 1.3 ‰ ($n = 9$). In addition, the average δ^{18}O-NO$_2$ value of filter samples collected in moderate T, varied RH conditions (1.3–77.7%) was 9.8 ± 1.0 ‰ ($n = 9$). Overall, this indicates that NO$_{2(g)}$ passive samplers perform well under moderate temperatures when compared with the reference gas tank (Fig. 2), and indicates a < 1.5 ‰ precision for filter determinations of both δ^{15}N-NO$_2$ and δ^{18}O-NO$_2$ values under varied RH conditions. However, the higher standard deviation for the varied RH conditions (± 1.3 ‰) than for the varied T, low RH condition collections (± 0.4 ‰) further demonstrates the RH effect on passive sampler NO$_{2(g)}$ isotope collection. This effect is also suggested by the significant, positive correlation between relative humidity and both δ^{15}N-NO$_2$ and δ^{18}O-NO$_2$ values ($r^2 = 0.30$–0.31, $p < 0.01$; Fig. 3).

The mean δ^{15}N-NO$_2$ value from the reference gas tank was not statistically different from values from filter collections under moderate T, varied RH conditions ($p = 0.07$). Conversely, ANOVA tests conducted for this grouping (moderate T, varying RH) showed a difference amongst passive sampler δ^{15}N-NO$_2$ values ($p < 0.00001$). In addition, the p values (ANOVA) were <0.001 for collections under both high T, varied RH and low T, varied RH conditions. This indicates that the RH conditions influence passive sampler NO$_{2(g)}$ isotope collections because collections under the same temperature, but different RH conditions, result in statistically different δ^{15}N-NO$_2$ values.

Previous studies have concluded that moisture conditions are the most important environmental factor for the accurate performance of TEA-adsorbent samplers.[41] In low RH conditions, the lack of water vapor may not allow TEA to quantitatively convert trapped NO$_{2(g)}$ into NO$_2^-{}_{(aq)}$, and it has been confirmed that extremes in RH conditions have an observable effect on passive sampling rates.[41,59] Decreased RH conditions are likely inhibiting the uptake of NO$_{2(g)}$ which results in decreased concentrations, and, in turn, leads to variable δ^{15}N-NO$_2$ values. These results indicate that there is

an isotopic fractionation occurring due to RH conditions in the chamber, but combined effects from both temperature and RH conditions are important to consider.

Combined effects and modeled fractionation factors

To better understand the preferential diffusion of NO$_{2(g)}$ isotopes, the use of kinetic fractionation factors was explored. To determine the kinetic fractionation factors, an approximate fraction factor was determined using Eqn. (3):

$$\Delta = \delta_P - \delta_S \qquad (3)$$

where Δ is the approximate fractionation factor (‰), δ_P is the δ^{15}N-NO$_2$ value determined from the filter eluent (‰), and δ_S is the δ^{15}N-NO$_2$ value determined from the reference gas tank (‰). Using Δ, a kinetic fractionation factor was determined using Eqn. (4):

$$\alpha = \frac{\Delta}{1000} + 1 \qquad (4)$$

where α is the kinetic fractionation factor in terms of the kinetic rate constants (k) between the light N isotope (^{14}N) and heavy N isotope (^{15}N). There was a diffusive effect on the NO$_{2(g)}$ isotopes during sampler uptake for all filter collections under low RH conditions, as the kinetic fractionation factors were <1.0. The kinetic fractionation factors from all filter collections above 1.3% RH were >1.0, except when RH was 78% (0.9995). Under both low and high RH conditions, ^{15}N was preferentially adsorbed to the filter and converted into NO$_2^-{}_{(aq)}$. Due to the lack of water vapor in the chamber under low RH conditions, TEA-coated filters may not quantitatively convert ^{14}N as effectively as ^{15}N, and isotopic interactions with water vapor may be influencing collections under high RH conditions. Further exploration into the gaseous diffusion rates of ^{14}N and ^{15}N of NO$_{2(g)}$ in air, under different RH conditions, would provide more detail for sampling NO$_{2(g)}$ isotopes, but exploration of these dynamics was beyond the scope of this study.
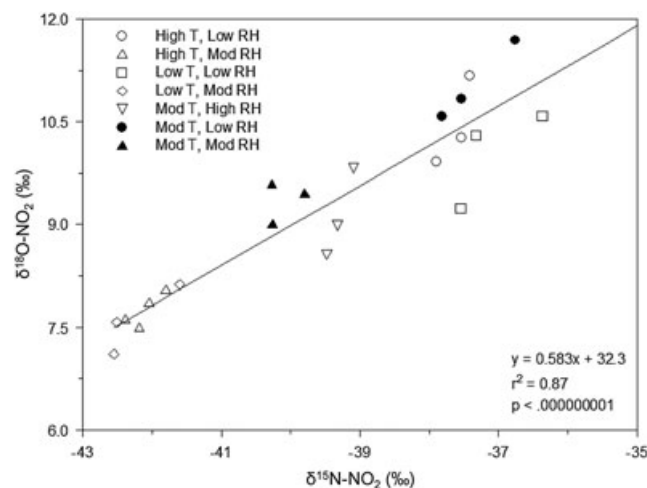

Figure 4. δ^{15}N-NO$_2$ values vs. δ^{18}O-NO$_2$ values from filter NO$_{2(g)}$ collections. Different environmental conditions are denoted by different symbols and the solid line is the linear regression line.

The δ^{15}N-NO$_2$ and δ^{18}O-NO$_2$ values from filter-collected NO$_{2(g)}$ under all environmental conditions were compared with each other and showed a positive, significantly correlated relationship ($r^2 = 0.87$, $p < 0.00001$; Fig. 4). Kinetic fractionation effects from RH conditions were observed for both NO$_{2(g)}$ isotopes, leading to a strong correlation. The combined environmental effect on NO$_{2(g)}$ isotopes during diffusion processes under different environmental conditions was explored by modeling fractionation factors at a range of environmental conditions. An approximate fractionation factor was determined for every filter δ^{15}N-NO$_2$ value using Eqn. (3). A multiple regression was then run on approximate fractionation factors from the filter samples using RH and T as independent variables. Turbulence was not used because it could not be converted into a wind speed variable that is applicable for field conditions. The multiple regression had an adjusted r^2 of 0.33 ($p < 0.01$) and the resulting equation was:

$$\Delta_F = -3.423 + 0.045*RH_M + 0.081*T_M \qquad (5)$$

where Δ_F is the approximate fractionation factor (‰), RH$_M$ is the average measured RH (%), and T$_M$ is the average measured temperature (°C). Using this equation, all combinations of possible RH conditions (0–100%) and all likely temperature conditions (°C) for sampler deployments (0–40°C) were input to determine approximate fractionation factors using different RH/T combinations (Fig. 5). This analysis indicates that likely environmental conditions for passive sampler deployments (average RH of 20–90%, average T of 0–30°C) will normally yield ≤1–2 ‰ fractionations (Fig. 5). Further inter-calibration studies are needed to determine whether field conditions support this evidence.

Overall accuracy and precision

The average δ^{15}N-NO$_2$ values determined from all the filter samples ($n = 21$) are in good agreement with the δ^{15}N-NO$_2$ values determined from the reference gas tank ($n = 3$). While
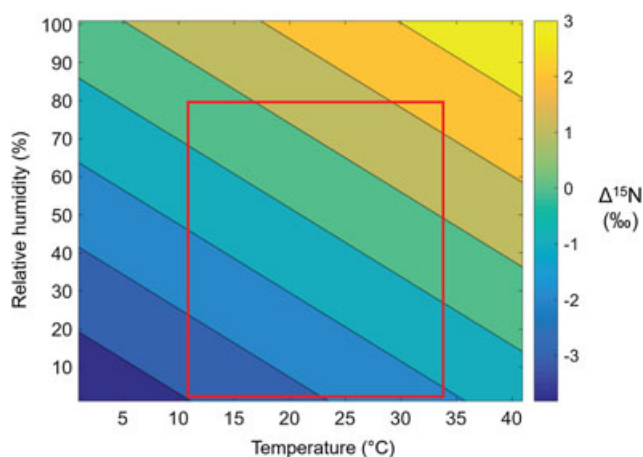
there was a statistically significant difference in the mean δ^{15}N-NO$_2$ values between the two collection methods, the difference was quantifiable and was attributable to RH variations. Temperature effects on the δ^{15}N-NO$_2$ values from filter collections are believed to be minimal and the ~2.0 ‰ accuracy decrease at different temperatures was due to RH condition effects rather than temperature fluctuations. The δ^{15}N-NO$_2$ values from filter samples were most accurate (≤0.01% error) under 22–23°C, 33–78% RH conditions.

Overall, TEA-coated filters provide an accurate and precise method for the quantitative determination of δ^{15}N-NO$_2$ values from filters deployed in varied simulated environmental conditions with a ≤ 1–2 ‰ fractionation occurring under moderate RH conditions. Although extreme RH conditions can produce a larger isotopic fractionation, areas where passive samplers are likely to be used do not sustain 1% RH conditions (e.g., Death Valley, CA, USA; Avg. RH = ~10–50%) and high precipitation areas do not always sustain extremely high RH conditions (e.g., Seattle, WA, USA; Avg. RH ~60–90%).

TEA-coated filters provide a precise method for determining δ^{18}O-NO$_2$ values from atmospheric NO$_{2(g)}$. The overall accuracy and precision of the method for δ^{15}N-NO$_2$ values are ≤2.1 ‰, which is comparable with other NO$_x$ isotope collection methods (precision of ±1.5 ‰).[15] In addition, the precision of individual filter collections under the same conditions for both δ^{15}N-NO$_2$ and δ^{18}O-NO$_2$ values is ≤0.6 ‰, which is near the standard deviation for isotope analysis reference standards (≤0.25 ‰ and ≤0.5 ‰ for δ^{15}N-NO$_2$ and δ^{18}O-NO$_2$ values, respectively). Experiments conducted under realistic environmental field conditions for filter deployments (average RH of 20–90%, average T of 0–30°C) had an accuracy and precision of ≤1.5 ‰ for δ^{15}N-NO$_2$ values. The overall precision of the method for δ^{18}O-NO$_2$ values is ±1.3 ‰. We observed environmental effects in the δ^{15}N-NO$_2$ and δ^{18}O-NO$_2$ values because of variations in RH conditions and this fractionation should be considered in future studies. Future research should investigate method inter-comparisons between passive samplers and other methods (e.g., denuder tubes or aqueous collection solutions) under field conditions; this will provide further inter-calibration of δ^{15}N-NO$_2$ determination methods.

CONCLUSIONS

This study quantitatively evaluates the use of a passive Ogawa NO$_{2(g)}$ sampler for isotopic composition determination under varied environmental conditions. Experiments conducted under realistic environmental field conditions for filter deployments had an overall accuracy and precision of ≤2.1 ‰ for δ^{15}N-NO$_2$ values; individual experiments had a precision of ≤0.6 ‰ for δ^{15}N-NO$_2$ values, and an overall precision of ±1.3 ‰ for δ^{18}O-NO$_2$ values. This study provides a proof of concept for this method using highly simulated environments and under well-mixed conditions, provides a quantified accuracy for the method, and provides the first approximation to predict environmentally caused fractionations for subsequent isotope studies using passive samplers. Our results display the potential for minor NO$_{2(g)}$ isotope fractionation under environmental conditions with extremely low/high

Figure 5. Approximate fractionation factors of δ^{15}N-NO$_2$ values at corresponding temperatures and relative humidities. Different intervals of approximate fractionation factors are denoted by the blue to yellow interval scale and the internal red outlined box denotes environmental conditions used in this study. [Color figure can be viewed at wileyonlinelibrary.com]

temperatures or relative humidities. Since, however, δ^{15}N-NO$_x$ values from anthropogenic and natural sources are so wide-ranging (–49 to +26 ‰),[13–23] these minor fractionations should not have a large effect when determining source apportionments. Future studies into passive sampler determination of δ^{15}N-NO$_2$ and δ^{18}O-NO$_2$ values should investigate low concentration environments and further evaluate inter-comparisons between methods in field conditions, executed over similar temporal resolutions, to further constrain the accuracy and precision of this and other methods.

Acknowledgments

REFERENCES

[1] D. Solomon, S. M. Qin, Z. Manning, M. Chen, K. B. Marquis, M. T. Averyt, Miller HL, S. Solomon, D. Qin, M. Manning, Z. Chen, M. Marquis, K. B. Averyt, M. Tignor, H. L. Miller, Summary for Policymakers, in *Climate Change 2007: The Physical Science Basis. Contribution of Working Group I to the Fourth Assessment Report of the Intergovernmental Panel on Climate Change*. Cambridge University Press, New York, **2007**, p. 996.

[2] P. J. Crutzen. The role of NO and NO$_2$ in the chemistry of the troposphere and stratosphere. *Annu. Rev. Earth Planet. Sci.* **1979**, *7*, 443.

[3] P. A. Leighton. *Photochemistry of Air Pollution*. Academic Press, New York, **1961**.

[4] P. J. Crutzen, P. H. Zimmerman. The changing photochemistry of the troposphere. *Tellus B* **1991**, *43*, 136.

[5] M. G. Lawrence, P. J. Crutzen. Influence of NOx emissions from ships on tropospheric photochemistry and climate. *Nature* **1999**, *402*, 167.

[6] R. Ehrlich, J. C. Findlay, J. D. Fenters, D. E. Gardner. Health effects of short-term inhalation of nitrogen dioxide and ozone mixtures. *Environ. Res.* **1977**, *14*, 223.

[7] M. Kampa, E. Castanas. Human health effects of air pollution. *Environ. Pollut.* **2008**, *151*, 362.

[8] J. Harju, A. Winnberg, J. G. A. Wouterloot. The distribution of OH in Taurus Molecular Cloud-1. *Astron. Astrophys.* **2000**, *1065*.

[9] J. N. Galloway, F. J. Dentener, D. G. Capone, E. W. Boyer, R. W. Howarth, S. P. Seitzinger, G. P. Asner, C. C. Cleveland, P. A. Green, E. A. Holland, D. M. Karl, A. F. Michaels, J. H. Porter, A. R. Townsend, C.J. Vörösmarty. Nitrogen cycles: Past, present, and future. *Biogeochemistry* **2004**, *70*, 153.

[10] L. Zhang, D. J. Jacob, E. M. Knipping, N. Kumar, J. W. Munger, C. C. Carouge, A. Van Donkelaar, Y. X. Wang, D. Chen. Nitrogen deposition to the United States: Distribution, sources, and processes. *Atmos. Chem. Phys.* **2012**, *12*, 4539.

[11] S. Reis, R. W. Pinder, M. Zhang, G. Lijie, M. A. Sutton. Reactive nitrogen in atmospheric emission inventories. *Atmos. Chem. Phys.* **2009**, *9*, 7657.

[12] L. Jaeglé, L. Steinberger, R. V. Martin, K. Chance. Global partitioning of NOx sources using satellite observations: relative roles of fossil fuel combustion, biomass burning and soil emissions. *Faraday Discuss.* **2005**, *130*, 407.

[13] W. W. Walters, B. D. Tharp, H. Fang, B. J. Kozak, G. Michalski. Nitrogen isotope composition of thermally produced NO$_x$ from various fossil-fuel combustion sources. *Environ. Sci. Technol.* **2015**, *49*, 11363.

[14] W. W. Walters, S. R. Goodwin, G. Michalski. Nitrogen stable isotope composition (δ^{15}N) of vehicle-emitted NO$_x$. *Environ. Sci. Technol.* **2015**, *49*, 2278.

[15] D. L. Fibiger, M. G. Hastings, A. F. Lew, R. E. Peltier. Collection of NO and NO$_2$ for isotopic analysis of NO$_x$ emissions. *Anal. Chem.* **2014**, *86*, 12115.

[16] J. D. Felix, E. M. Elliott, S. L. Shaw. Nitrogen isotopic composition of coal-fired power plant NO$_x$: Influence of emission controls and implications for global emission inventories. *Environ. Sci. Technol.* **2012**, *46*, 3528.

[17] J. D. Felix, E. M. Elliott. Isotopic composition of passively collected nitrogen dioxide emissions: Vehicle, soil and livestock source signatures. *Atmos. Environ.* **2014**, *92*, 359.

[18] T. H. E. Heaton. ^{15}N/^{14}N ratios of NO$_x$ from vehicle engines and coal-fired power stations. *Tellus B* **1990**, *42B*, 304.

[19] M. Ammann, R. Siegwolf, F. Pichlmayer, M. Suter, M. Saurer, C. Brunold. Estimating the uptake of traffic-derived NO$_2$ from ^{15}N abundance in Norway spruce needles. *Oecologia* **1999**, *118*, 124.

[20] D. Li, X. Wang. Nitrogen isotopic signature of soil-released nitric oxide (NO) after fertilizer application. *Atmos. Environ.* **2008**, *42*, 4747.

[21] H. Moore. The isotopic composition of ammonia, nitrogen dioxide and nitrate in the atmosphere. *Atmos. Environ.* **1977**, *11*, 1239.

[22] J. Pearson, D. M. Wells, K. J. Seller, A. Bennett, A. Soares, J. Woodall, M. J. Ingrouille. Traffic exposure increases natural ^{15}N and heavy metal concentrations in mosses. *New Phytol.* **2000**, *147*, 317.

[23] T. Hoering. The isotopic composition of the ammonia and the nitrate ion in rain. *Geochim. Cosmochim. Acta* **1957**, *12*, 97.

[24] W. W. Walters, G. Michalski. Theoretical calculation of nitrogen isotope equilibrium exchange fractionation factors for various NO$_y$ molecules. *Geochim. Cosmochim. Acta* **2015**, *164*, 284.

[25] W. W. Walters, G. Michalski. Theoretical calculation of oxygen equilibrium isotope fractionation factors involving various NO$_y$ molecules, OH, and H$_2$O and its implications for isotope variations in atmospheric nitrate. *Geochim. Cosmochim. Acta* **2016**, *191*, 89.

[26] W. W. Walters, D. S. Simonini, G. Michalski. Nitrogen isotope exchange between NO and NO$_2$ and its implications for δ^{15}N variations in tropospheric NO$_x$ and atmospheric nitrate. *Geophys. Res. Lett.* **2016**, *43*, 440.

[27] E. M. Elliott, C. Kendall, E. W. Boyer, D. A. Burns, G. G. Lear, H. E. Golden, K. Harlin, A. Bytnerowicz, T. J. Butler, R. Glatz. Dual nitrate isotopes in dry deposition: Utility for partitioning NO$_x$ source contributions to landscape nitrogen deposition. *J. Geophys. Res. Biogeosciences* **2009**, *114*, 1.

[28] E. M. Elliott, C. Kendall, S. D. Wankel, D. A. Burns, E. W. Boyer, K. Harlin, D. J. Bain, T. J. Butler. Nitrogen isotopes as indicators of NO_x source contributions to atmospheric nitrate deposition across the midwestern and northeastern United States. *Environ. Sci. Technol.* **2007**, *41*, 7661.

[29] M. G. Hastings. Isotopic evidence for source changes of nitrate in rain at Bermuda. *J. Geophys. Res.* **2003**, *108*, 1.

[30] M. G. Hastings, E. J. Steig, D. M. Sigman. Seasonal variations in N and O isotopes of nitrate in snow at Summit, Greenland: Implications for the study of nitrate in snow and ice cores. *J. Geophys. Res. D Atmos.* **2004**, 109, DOI https://doi.org/10.1029/2004JD004991.

[31] H. D. Freyer. Seasonal trends of NH_4^+ and NO_3^- nitrogen isotope composition in rain collected at Julich, Germany. *Tellus* **1978**, *30*, 83.

[32] H. D. Freyer. Seasonal-variation of $^{15}N/^{14}N$ ratios in atmospheric nitrate species. *Tellus Ser. B-Chemical Phys. Meteorol.* **1991**, *43*, 30.

[33] M. G. Hastings, J. C. Jarvis, E. J. Steig. Anthropogenic impacts on nitrogen isotopes of ice-core nitrate. *Science* **2009**, *324*, 1288.

[34] A. P. Wolfe, A. C. Van Gorp, J. S. Baron. Recent ecological and biogeochemical changes in alpine lakes of Rocky Mountain National Park (Colorado, USA): a response to anthropogenic. *Geobiology* **2003**, *1*, 153.

[35] A. P. Wolfe, J. S. Baron, R. J. Cornett. Anthropogenic nitrogen deposition induces rapid ecological changes in alpine lakes of the Colorado Front Range (USA). *J. Paleolimnol.* **2001**, *25*, 1.

[36] M. Saurer, P. Cherubini, M. Ammann, B. De Cinti, R. Siegwolf. First detection of nitrogen from NO_x in tree rings: A $^{15}N/^{14}N$ study near a motorway. *Atmos. Environ.* **2004**, *38*, 2779.

[37] H. D. Freyer, D. Kley, A. Volzthomas, K. Kobel. On the interaction of isotopic exchange processes with photochemical-reactions in atmospheric oxides of nitrogen. *J. Geophys. Res.* **1993**, *98*, 14791.

[38] K. Redling, E. Elliott, D. Bain, J. Sherwell. Highway contributions to reactive nitrogen deposition: Tracing the fate of vehicular NO_x using stable isotopes and plant biomonitors. *Biogeochemistry* **2013**, *116*, 261.

[39] P. M. Homyak, J. C. Blankinship, K. Marchus, D. M. Lucero, J. O. Sickman, J. P. Schimel. Aridity and plant uptake interact to make dryland soils hotspots for nitric oxide (NO) emissions. *Proc. Natl. Acad. Sci. USA* **2016**, *113*, E2608.

[40] B. Dahal, M. G. Hastings. Technical considerations for the use of passive samplers to quantify the isotopic composition of NO_x and NO_2 using the denitrifier method. *Atmos. Environ.* **2016**, *143*, 60.

[41] J. N. N. Cape. The use of passive diffusion tubes for measuring concentrations of nitrogen dioxide in air. *Crit. Rev. Anal. Chem.* **2009**, *39*, 289.

[42] H. Tang, T. Lau, B. Brassard, W. Cool. A new all-season passive sampling system for monitoring NO_2 in air. *Field Anal. Chem. Technol.* **1999**, *3*, 338.

[43] D. J. Moschandreas, S. M. Relwani, K. C. Taylor, J. D. Mulik. A laboratory evaluation of a nitrogen dioxide personal sampling device. *Atmos. Environ. Part A. Gen. Top.* **1990**, *24*, 2807.

[44] H. J. Moriske, M. Schondube, G. Ebert, G. Menk, B. Seifert, H. J. Abraham. Measurements of NO_2 concentrations in the air using passive Palmes samplers. 2. Field studies. *Gefahrstoffe Reinhaltung Der Luft* **1996**, *56*, 161.

[45] J. David Felix, E. M. Elliott, T. J. Gish, L. L. McConnell, S. L. Shaw. Characterizing the isotopic composition of atmospheric ammonia emission sources using passive samplers and a combined oxidation-bacterial denitrifier approach. *Rapid Commun. Mass Spectrom.* **2013**, *27*, 2239.

[46] H. E. Golden, E. W. Boyer, M. G. Brown, E. M. Elliott, D. K. Lee. Simple approaches for measuring dry atmospheric nitrogen deposition to watersheds. *Water Resour. Res.* **2008**, *44*, W00d02. https://doi.org/10.1029/2008WR006952.

[47] M. A. Puchalski, M. E. Sather, J. T. Walker, C. M. B. Lehmann, D. A. Gay, J. Mathew, W. P. Robarge. Passive ammonia monitoring in the United States: Comparing three different sampling devices. *J. Environ. Monit.* **2011**, *13*, 3156.

[48] Y. S. Tang, J. N. Cape, M. A. Sutton. Development and types of passive samplers for monitoring atmospheric NO_2 and NH_3 concentrations. *ScientificWorldJournal* **2001**, *1*, 513.

[49] *NO, NO_2, NO_x and SO_2 Sampling Protocol Using the Ogawa Sampler*. Ogawa & Company, **2006**.

[50] *Determination of Nitrogen Oxide Emissions from Stationary Sources*. EPA, **2010**.

[51] D. M. Sigman, K. L. Casciotti, M. Andreani, C. Barford, M. Galanter, J. K. Böhlke. A bacterial method for the nitrogen isotopic analysis of nitrate in seawater and freshwater. *Anal. Chem.* **2001**, *73*, 4145.

[52] K. L. Casciotti, D. M. Sigman, M. G. Hastings, J. K. Böhlke, A. Hilkert. Measurement of the oxygen isotopic composition of nitrate in seawater and freshwater using the denitrifier method. *Anal. Chem.* **2002**, *74*, 4905.

[53] K. L. Casciotti, J. K. Böhlke, M. R. McIlvin, S. J. Mroczkowski, J. E. Hannon. Oxygen isotopes in nitrite: Analysis, calibration, and equilibration. *Anal. Chem.* **2007**, *79*, 2427.

[54] TIBCO. Spotfire S+® 8.2, **2010**.

[55] A. J. Gair, S. A. Penkett. The effects of wind speed and turbulence on the performance of diffusion tube samplers. *Atmos. Environ.* **1995**, *29*, 2529.

[56] N. A. Martin, J. J. Helmore, S. White, I. L. Barker Snook, A. Parish, L. S. Gates. Measurement of nitrogen dioxide diffusive sampling rates for Palmes diffusion tubes using a controlled atmosphere test facility (CATFAC). *Atmos. Environ.* **2014**, *94*, 529.

[57] M. R. Heal, M. A. O'Donoghue, J. N. Cape. Overestimation of urban nitrogen dioxide by passive diffusion tubes: A comparative exposure and model study. *Atmos. Environ.* **1999**, *33*, 513.

[58] H. Plaisance, A. Piechocki-Minguy, S. Garcia-Fouque, J. C. Galloo. Influence of meteorological factors on the NO_2 measurements by passive diffusion tube. *Atmos. Environ.* **2004**, *38*, 573.

[59] T. S. Hansen, M. Kruse, H. Nissen, M. Glasius, C. Lohse. Measurements of nitrogen dioxide in Greenland using Palmes diffusion tubes. *J. Environ. Monit.* **2001**, *3*, 139.